



Modeling of the swelling–shrinkage behavior of expansive clays during wetting–drying cycles

N. F. Zhao¹ · W. M. Ye^{1,2} · B. Chen¹ · Y. G. Chen^{1,2} · Y. J. Cui^{1,3}

Received: 10 December 2017 / Accepted: 10 September 2018 / Published online: 13 October 2018
© Springer-Verlag GmbH Germany, part of Springer Nature 2018

Abstract

This paper presents a constitutive model for simulating the swelling–shrinkage volume change of expansive soils during wetting–drying cycles. Based on the concept of the critical swelling–shrinkage state proposed by Zhao et al. [21], the elastic swelling–shrinkage deformation, plastic swelling/shrinkage deformation, and accumulative deformation during wetting–drying cycles were analyzed. Influences of the initial dry density and stress applied on the yield suction were discussed. The suction decreasing yield surface (SD) and suction increasing yield surface (SI) were defined. The variations of SD and SI yield surfaces were proposed. Calibration was performed with results of the cyclic wetting–drying tests conducted. The proposed model was validated by simulating cyclic wetting–drying tests conducted on compacted Gao-MiaoZi (GMZ) bentonite. Good agreements were obtained between the simulation results and the experimental ones. Using the proposed model, influences of dry density and stress applied on the swelling–shrinkage deformation and accumulative deformation of expansive soil were well described.

Keywords Constitutive model · Critical swelling–shrinkage state · Swelling stable state · Suction yield surface · Wetting–drying cycles · Swelling and shrinkage deformation

1 Introduction

Geotechnical problems induced by the effects of wetting–drying cycles due to the periodic climate changes or environmental variations are widely encountered in the environments [9, 10]. In deep geological repositories, working as buffer/backfill materials, compacted bentonite will experience large swelling–shrinkage deformations during the cyclically wetting and drying processes, due to the periodical variations in infiltration of ground water from surrounding rock and heat generated from the

radioactive waste in the canister [18]. This kind of swelling–shrinkage deformations causes increase in permeability even possible leakage of nuclides from the canister [4, 19]. In the meantime, swelling–shrinkage deformations of expansive soil foundations also could be observed due to the cyclic wetting and drying induced by the seasonal variations of groundwater level, which consequently lead to destructions of buildings and structures in expansive soil area [6]. Similarly, swelling–shrinkage deformations in the cyclically wetting and drying processes induced by periodic rainfall and evaporations in expansive soil slope, leading to decrease in soil strength even failure of soil slope [14]. Therefore, investigations on the volume change behavior of expansive clay induced by drying–wetting cycles including development of constitutive models for describing the swelling–shrinkage deformation of expansive soil are of great theoretic and practical importance.

In this respect, many contributions have been made on investigations of swelling–shrinkage behavior of expansive clays through cyclic wetting–drying tests and construction of constitutive models. For cyclic wetting–drying tests, mainly two types of tests have been conducted including

✉ W. M. Ye
ye_tju@tongji.edu.cn

¹ Key Laboratory of Geotechnical and Underground Engineering of Ministry of Education, Tongji University, Shanghai 200092, China

² United Research Center for Urban Environment and Sustainable Development, the Ministry of Education, Shanghai 200092, China

³ Ecole des Ponts ParisTech, UR Navier/CERMES, 77455 Paris, France

cyclic suction-controlled tests [1, 4, 11, 12, 14] and alternately soaked-dried tests [5, 7, 15, 16]. According to the test results from the studies, common conclusions could be reached that [4, 17]: (i) The magnitude of swelling deformation increases with the increase in water content or the decrease in suction; similarly, the magnitude of shrinkage deformation increases with the decrease in water content or the increase in suction. (ii) The difference between swelling and shrinkage deformations in the wetting–drying cycles reaches its maximum value in the first cycle. Then, it decreases with the increase in wetting–drying cycles. (iii) Before reaching the equilibrium state, the accumulated (total) deformation is of swelling or shrinkage depending on soil properties, initial conditions, vertical stress or confining pressure, etc. (iv) The soil deformation reaches its equilibrium state after a certain number of wetting–drying cycles [13]; [20].

For the development of constitutive models, most of them were constructed based on elastoplastic theory, among which, the Barcelona Basic Model (BBM) and Barcelona Expansive Model (BExM) are the most representative ones.

During the wetting–drying cycles, the variation of swelling–shrinkage deformation is induced by change of suction. The total deformation including the elastic deformation and plastic deformation is expressed as Eq. (1).

$$de = de^e + de^p \quad (1)$$

where de is the total deformation, the de^e and de^p represent the elastic and plastic deformations, respectively.

The elastic deformations occur when the current suction is smaller than the yield suction. Contrarily, the plastic deformations occur. In this regard, the elastic deformations and the plastic deformations can be calculated by the following equations [2].

$$\begin{cases} de_{vs}^e = \kappa_s \frac{ds}{s + p_{at}} \\ de_{vs}^p = \lambda_s \frac{ds_0}{s_0 + p_{at}} \end{cases} \quad (2)$$

where κ_s and λ_s are the elastic and plastic stiffness parameters changing with suction, respectively. S_0 is the yield suction.

According to Eq. (2), there are three key issues (including the type of suction yield surface, variation of suction yield surface (the hardening law) and the calibration on the elastic and plastic stiffness parameters with changing suction) to be solved. In this regard, BBM model [2] and BExM model [3, 4, 8] were proposed.

In BBM model [2], equations for the suction yield surface and its variation were proposed for describing the swelling–shrinkage deformation. However, only elastic behavior of unsaturated soil during wetting is described in this model,

which is almost impossible to reflect the accumulative swelling deformation of dense soils after experiencing wetting–drying cycles under lower stress. Meanwhile, yield suction is constant with the changes of the stress applied. It is also almost impossible to reflect the vertical stress and confining stress effects on the swelling–shrinkage deformation.

In the BExM model [3, 4, 8], concepts of the suction decreasing yield surface (SD) and suction increasing yield surface (SI) were introduced for analyzing the swelling and shrinkage mechanisms. However, functions for two the suction yield surfaces (SD and SI) are not identified, and variations of the two suction yield surfaces are also not described. Eventually, swelling–shrinkage deformations are calculated by two empirical functions (fI and fD), which are fitted by back analysis of related test results. Moreover, the parameters in the two empirical functions are also difficult to be determined [17].

In this study, based on the concept of the critical swelling–shrinkage state proposed by Zhao et al. [20], the elastic swelling–shrinkage deformation, plastic swelling–shrinkage deformation and accumulative deformation during the wetting–drying cycles were analyzed. The effects of dry density and the stress applied on the yield suction were discussed. Suction decreasing yield surface (SD) and suction increasing yield surface (SI) were defined, and then, the variations of SD and SI yield surfaces were proposed. Based on these, an elastoplastic constitutive model was proposed for describing the swelling–shrinkage volume change behavior of compacted expansive clays. The proposed model was verified using the cyclical wetting–drying test results conducted on compacted GaoMiaoZi (GMZ) bentonite.

2 Model framework

2.1 The critical swelling–shrinkage line

According to cyclic wetting and drying test results [20], the following conclusions could be reached. (1) After several wetting–drying cycles, the swelling deformation in the wetting processes is equal to the shrinkage deformation in the corresponding drying process, leading to elastic deformations in the wetting–drying cycles. Consequently, soil reaches an equilibrium state (A_1A_2 , B_1B_2 and C_1C_2 in Fig. 1). (2) For soils with same initial dry densities, accumulative swelling deformation occurs under smaller applied stresses; while an accumulative shrinkage deformation was obtained under larger applied stresses. Therefore, it must exist a critical stress when the accumulative deformation is equal to zero. (3) For the soils with different dry densities tested under a same applied stress, accumulative swelling deformation was obtained on the soils with larger dry densities, while accumulative shrinkage

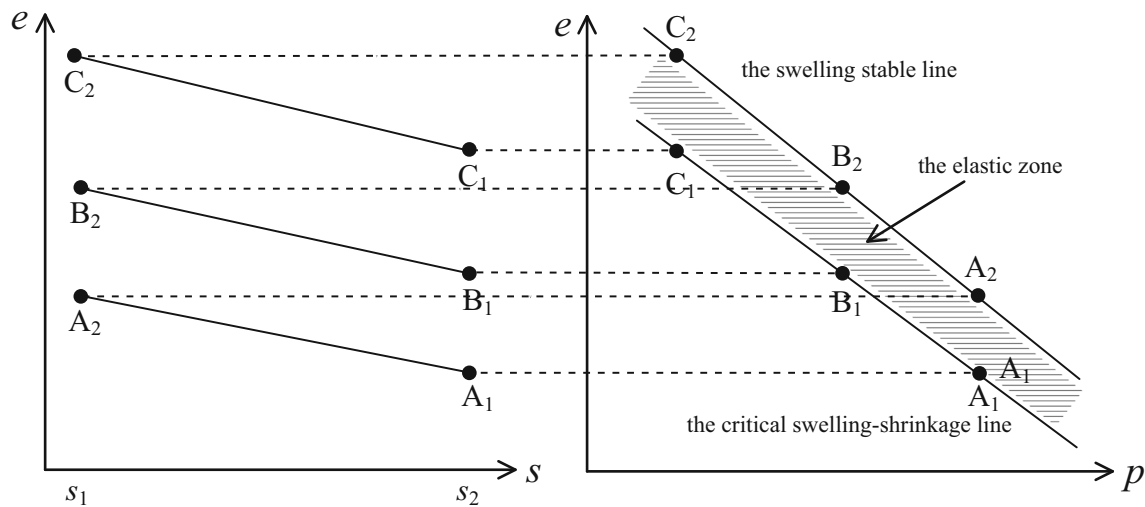


Fig. 1 CSSL, SSL, and the elastic zone

deformation was recorded for those with smaller dry densities. Therefore, it must exist a critical dry density when the accumulative deformation is zero. (4) In the e - p space, the critical points, including the critical stress and critical void ratio, can be determined (points A_1 , B_1 and C_1 in Fig. 1). All the critical points almost locate in a line, which is defined as the critical swelling–shrinkage line (CSSL).

The critical swelling–shrinkage line has two meanings. (1) If a soil reaches the critical swelling–shrinkage state, no accumulative deformation occurs in the cyclic wetting–drying process. (2) If a soil reaches the critical swelling–shrinkage state, an elastic swelling–shrinkage deformation occurs in the wetting–drying cycles.

The equation for description of the critical swelling–shrinkage line can be defined as,

$$e_{cs} = \lambda_{cs}(p_{cs} - p_{re}) + e_{rc} \tag{3}$$

where e_{cs} is the critical swelling–shrinkage void ratio, p_{cs} is the critical swelling–shrinkage stress. Parameters λ_{cs} and e_{rc} are the slope and intercept of the critical line, respectively.

2.2 The swelling stable line

If a soil reaches the critical swelling–shrinkage state, the state (point A_2 , B_2 or C_2 in Fig. 1) at the end of the wetting path is defined as the swelling stable state. All the swelling stable state points locate on a straight line, which is defined as the swelling stable line (SSL).

Equation for describing the swelling stable line could be defined as,

$$e_{ss} = \lambda_{ss}p_{ss} + e_{rs} \tag{4}$$

where e_{ss} is the void ratio corresponding to the critical swelling stable state, p_{ss} is the critical swelling

stable stress. Parameters λ_{ss} are e_{rs} the slope and intercept of the critical swelling stable line, respectively.

2.3 The elastic zone

The specific zone enveloped by the critical swelling–shrinkage line and swelling stable line is defined as the elastic zone (Fig. 1). With the concept of the elastic zone, the relationship between the elastic compressibility coefficient and the applied stress can be reasonably obtained.

2.4 State parameter ψ

For describing the relationship of the current state and the critical state of a soil, a state parameter ψ is defined (Fig. 2). The parameter ψ can be used as a state indicator for determination of the relationship between the current state and the critical swelling–shrinkage state of soil with

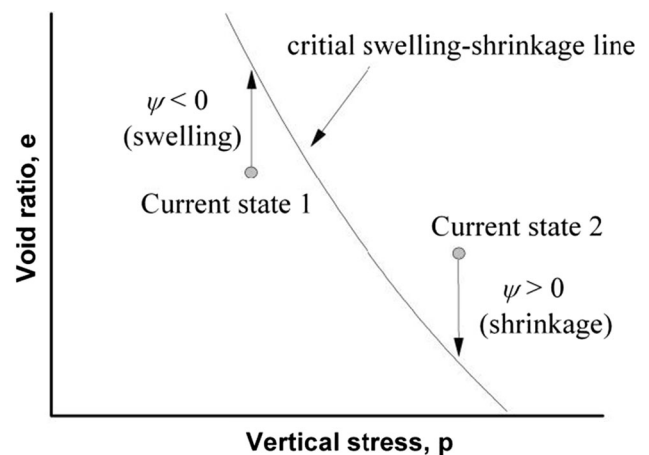


Fig. 2 State parameter ψ

consideration of coupling effects of dry density and the applied stress. If $\psi < 0$, the soil is in a dense state and accumulative swelling deformation occurs. If $\psi > 0$, the soil is in a loose state and accumulative shrinkage deformations occur. The state parameter also represents the total accumulative swelling/shrinkage deformation during several wetting–drying cycles.

According to the definition and Eq. (1), the state parameter ψ can be expressed as,

$$\psi = e - e_{cs} = e - [e_{rc} - \lambda_{cs}p_{cs}] \tag{5}$$

where e is the current void ratio and e_{cs} is the critical void ratio.

2.5 The suction yield surfaces

For describing the elastoplastic deformation and yield behavior of soil during wetting process, the yield suction is defined as the suction that soil transfers from an elastic state to the plastic one. During wetting process, the yield locus in the p - s space is defined as the suction decreasing yield surface (SD). Similarity, during drying process, the yield locus in the p - s space is defined as the suction increasing yield surface (SI).

1. The suction decreasing yield surface SD

For describing the suction decreasing yield surface (SD), it is assumed that there are five possible states A, B, C, D and E of a soil at the beginning of the wetting process as shown in Fig. 3. In Fig. 3, state A locates on the critical swelling–shrinkage line; it indicates that some elastic swelling deformation occurs during the wetting process. Therefore, for soil at state A, the yield suction is suction s_2 . This conclusion is consistent with that reported by Airò Farulla et al. [1]. However, for the state B, the applied

stress is smaller than the critical stress. Therefore, plastic swelling deformations occur during the wetting process. For soil at state B, their yield suction (S_{DB}) should be larger than s_2 . Similarly, for soil at state C, their state parameter is larger than that of soil at state B. The plastic swelling deformation is larger than that of soil at state B. Similar experimental observations were also reported by Nowamooz and Masrouri [13] and Zhao et al. [20]. Therefore, the suction S_{DC} is larger than suction S_{DB} .

For soil at state D, swelling deformation is less than that of soil at state C. It indicates that smaller plastic deformations occur during the wetting process. The yield suction S_{DD} is also larger than s_2 . For soil locates at state E, swelling deformation is less than that of soils locate at state D indicating that smaller plastic deformations occur during the wetting processes. The yield suction S_{DE} is also larger than S_{DD} .

Therefore, for the applied stress lower than the critical stress, the yield suction decreases as the applied stress increases. When the applied stress is equal to the critical stress, the yield suction is equal to the minimum value s_2 . If the applied stress higher than the critical stress, the yield suction increases as the stress applied increases.

It should be noted that, for simplification, a linear yield locus was adopted in this work for describing the suction decreasing yield surface (SD) (Fig. 3). The equation for suction decreasing yield surface (SD) can be expressed as,

$$s_D = \begin{cases} \frac{s_2 - s_1}{p_{cs} - p_{ref}} p + \frac{p_{cs}s_1 - p_{ref}s_2}{p_{cs} - p_{ref}} & (p \leq p_{cs}) \\ \frac{s_2 - s_1}{p_{cs} - p_c} p - \frac{p_{cs}s_1 - p_c s_2}{p_{cs} - p_c} & (p \geq p_{cs}) \end{cases} \tag{6}$$

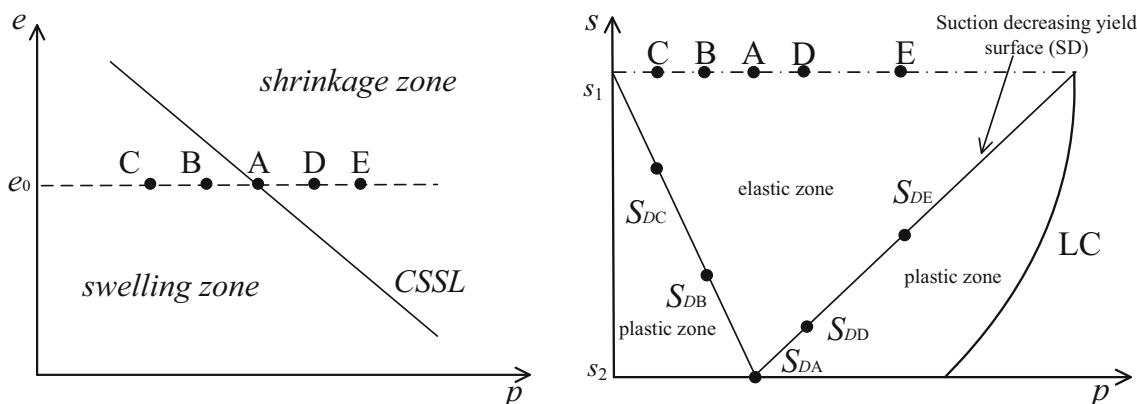


Fig. 3 Suction decreasing yield loci

where s_1 and s_2 are the highest and lowest suctions of the wetting and drying cycles processed. p is the vertical stress. p_{cs} is the critical stress. p_c is the yield stress of the soil with a suction of s_1 . p_{ref} is the reference stress, which is usually assumed to be 1 kPa.

2. Suction increasing yield surface SI

Similarly, for describing the suction increasing yield surface (SI), it is also assumed that there are five possible states A, B, C, D, and E of a soil at the beginning of drying processes as shown in Fig. 4.

In Fig. 4, state A locates on the stable line, it indicates that elastic shrinkage deformations occur during the drying process. Therefore, for a soil at state A, its yield suction is s_1 . However, for a soil at state B, the stress applied is smaller than the critical stable stress. Therefore, plastic shrinkage deformations occur during the drying process. For a soil at state B, the yield suction S_{IB} should be smaller than s_1 . Similarly, for a soil at state C, the state parameter is larger than that of a soil at state B. The plastic deformation is larger than that of soil at state B. Therefore, the suction S_{IC} is smaller than S_{IB} .

For a soil locate at state D, shrinkage deformation is less than that of soil at state C. It indicates that smaller plastic deformations occur during the drying process. The yield suction S_{DD} is also smaller than s_1 . The yield suction S_{DD} is also smaller than s_1 . For a soil locates at state E, shrinkage deformations are less than that of a soil locate at state D. It indicates that larger plastic deformations occur during the drying processes. The yield suction S_{IE} is also smaller than S_{ID} .

Therefore, for the applied stress lower than the critical stress, the yield suction increases as the applied stress increases. When the applied stress is equal to the critical stress, the yield suction is equal to the maximum value s_1 .

For the applied stress higher than the critical stress, the yield suction decreases as the stress applied increases.

Similarly, linear yield locus was also adopted in this work for describing the suction increasing yield surface (SI) (Fig. 4). The equation for suction increasing yield surface (SI) can be expressed as,

$$s_I = \begin{cases} \frac{s_2 - s_1}{p_{ss} - p_c} p + \frac{p_{ss}s_1 - p_{ref}s_2}{p_{ss} - p_c} & (p \leq p_{ss}) \\ \frac{p_{ss} - p_{ref}}{p_{ss} - p_c} p - \frac{p_{cs} - p_{ref}}{p_{ss} - p_c} & (p \geq p_{ss}) \end{cases} \quad (7)$$

where p_{ss} is the swelling stable stress. p_c is the yield stress of the soil with a suction of s_2 .

2.6 The evolution of the three yield surfaces

For describing the variations of suction decreasing yield surface (SD) during wetting–drying cycles, it is assumed that there is a soil at its initial state A0 locating in the swelling zone (Fig. 5a). Correspondingly, its initial suction decreasing yield surface (SD0) is given in Fig. 5c. After one wetting–drying cycle, the accumulative swelling deformations occur (Fig. 5b) and the current state moves to A1, which also locates in the swelling zone. However, the state parameter of A1 becomes smaller with the critical swelling–shrinkage stress decreased indicating that the suction decreasing yield surface shifts to left (Fig. 5c). Similarly, after several wetting–drying cycles, the current state changes to An, which locates on the critical swelling–shrinkage line. Then, only some elastic swelling–shrinkage deformations occur during the wetting–drying cycles (Fig. 5b), and then the suction decreasing yield surface (SD) stops to move (Fig. 5c).

Based on the above analysis, the variation of suction decreasing yield surface (SD) is depended on the variation of critical swelling–shrinkage stress and yield stress. Therefore, the critical swelling–shrinkage stress and yield

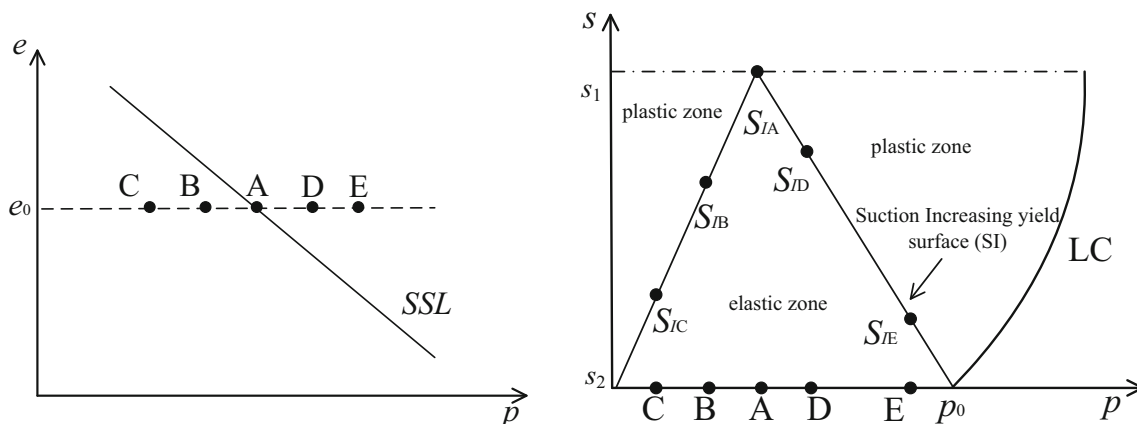


Fig. 4 Suction increasing yield loci

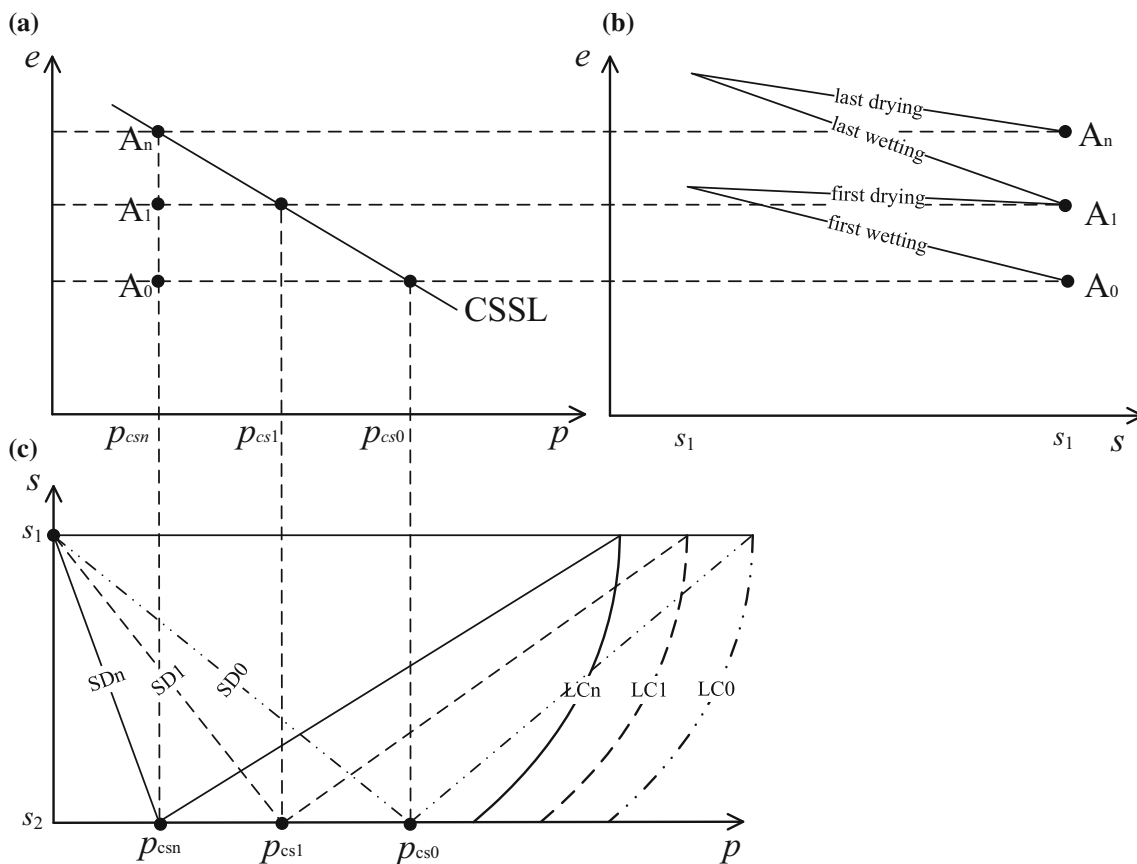


Fig. 5 Schematic evolution of SD

stress can be defined as hardening parameter. The critical swelling–shrinkage stress could be determined by the relationship between the equation of critical swelling–shrinkage line and the current void ratio. The yield stress could be obtained by the relationship between compression line and swelling line in the oedometer test with constant suction s_1 . The equations for the critical swelling–shrinkage stress and the yield stress could be expressed as:

$$\begin{cases} p_{cs} = \frac{e_{cs} - e_{rc}}{\lambda_{cs}} + p_{re} \\ p_c = \frac{\kappa_{s1}}{\kappa_{s1} - \lambda_{s1}} \left(\frac{N_{s1} - e}{\lambda_{s1}} + p_{ref} \right) - \frac{\lambda_{s1}}{\kappa_{s1} - \lambda_{s1}} p \end{cases} \quad (8)$$

For describing the variations of the suction increasing yield surface (SI) during the wetting–drying cycles, it is assumed that there is a soil at initial state $A_{0.5}$ in the shrinkage zone (Fig. 6a), and then its initial suction increasing yield surface (SI0) could be expressed in Fig. 6c. After one wetting–drying cycle, the accumulative shrinkage deformations occur (Fig. 6b) and the current state moves to $A_{1.5}$, which also locates in the shrinkage zone. However, the state parameter of $A_{1.5}$ becomes smaller with the critical stress increases indicating that the suction increasing yield surface shifts to right (Fig. 6c).

Similarly, after several wetting–drying cycles, the current state changes to A_n , which locates on the swelling stable line. Then, only elastic swelling–shrinkage deformations occur during the wetting–drying cycles (Fig. 6b), and then the suction increasing yield surface (SI) could not move (Fig. 6c).

Based on the above analysis, the variation of suction increasing yield surface (SI) is depended on the variation of swelling stable stress and yield stress. Therefore, the swelling stable stress and yield stress could be defined as hardening parameter. The swelling stable stress could be determined by the relationship between the equation of swelling stable line and the current void ratio. The yield stress could be obtained by the relationship between compression line and swelling line in the oedometer test with constant suction s_2 . The equations for the critical swelling–shrinkage stress and yield stress could be expressed as:

$$\begin{cases} p_{cs} = \frac{e_{cs} - e_{rc}}{\lambda_{cs}} + p_{re} \\ p_c = \frac{\kappa_{s2}}{\kappa_{s2} - \lambda_{s2}} \left(\frac{N_{s2} - e}{\lambda_{s2}} + p_{ref} \right) - \frac{\lambda_{s2}}{\kappa_{s2} - \lambda_{s2}} p \end{cases} \quad (9)$$

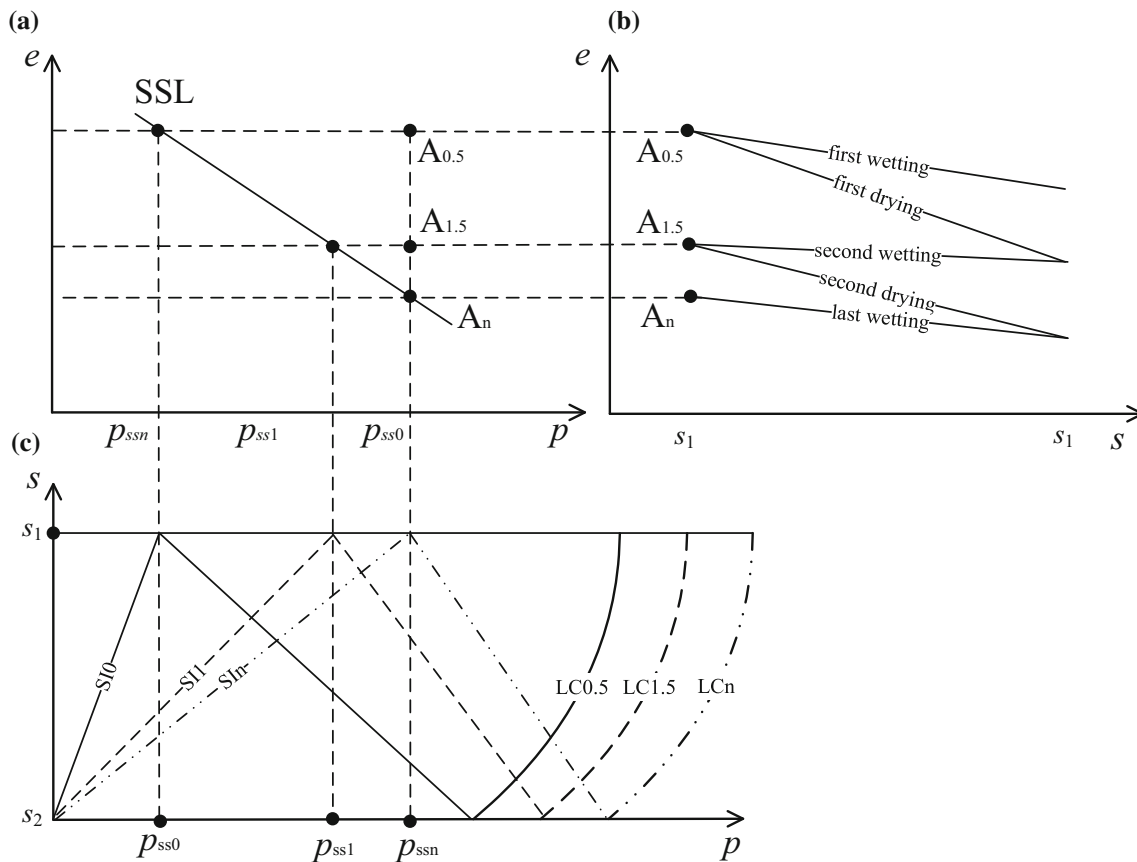


Fig. 6 Schematic evolution of SI

3 Calculation of swelling–shrinkage using the proposed model

To calculate the swelling–shrinkage deformations of the soil during the wetting–drying cycles, the initial state (p, s, e_0) of a soil, the critical swelling–shrinkage line and swelling stable line should be known. Then, the elastoplastic swelling deformation during the wetting process and the elastoplastic shrinkage deformation in the drying process can be calculated successively.

For calculation of the elastoplastic swelling deformation during the wetting process, according to the relationship between the initial state and critical swelling–shrinkage line, the critical stress is calculated by Eq. (3). In the meantime, the yield stress can be calculated by Eq. (8). Then, based on the critical stress and the yield stress calculated, the suction decreasing yield surface can be determined by Eq. (6). Then, based on the suction decreasing yield surface and current vertical stress, the yield suction can be calculated by Eq. (6). Meanwhile, combining to the critical swelling–shrinkage line and swelling stable line, the elastic compressibility coefficient can be calculated by Eq. (11). Then, based on the elastic compressibility coefficient and state parameter, the plastic compressibility

coefficient can be calculated by (12) and the elastoplastic swelling deformation can be calculated by Eq. (2). Finally, according to the initial state and swelling deformations calculated, the state of soil at the end of wetting process can be determined.

Simultaneously, for calculation of the elastoplastic shrinkage deformation during the drying process, according to the relationship between the state of soil at the end of wetting and swelling stable line, the swelling stable stress can be calculated by Eq. (4). In the meantime, the yield stress can be calculated by Eq. (9). Then, based on the swelling stable stress and yield stress, the equation for description of the suction increasing yield surface could be determined (Eq. (8)). Then, based on the suction increasing yield surface and current vertical stress, the yield suction can be calculated by Eq. (8). Meanwhile, combining to the elastic compressibility coefficient and state parameter, plastic compressibility coefficient can be calculated by (12). Finally, according to the state of soil at the end of the wetting process and the drying deformations calculated, the state of soil at the end of drying process can be determined.

The calculation processes mentioned above should be repeated for the next wetting and drying cycle until all the wetting and drying cycles texted are simulated.

4 Determination of Parameters

To calculate the swelling and shrinkage deformation of the soil, the yield suction, elastic and plastic compressibility coefficients should be determined using 10 parameters, which include six yield stress parameters and two critical state line and two critical stable line parameters in the proposed model in this work.

For determination of the six yield stress parameters, oedometer tests should be conducted at constant suction s_1 and constant suction s_2 , respectively. Based on the test results, compression lines and swelling lines can be determined. Then, parameters λ_{s1} and N_{s1} can be obtained from the slope and intercept of the compression line at constant suction (s_1), respectively. Parameter κ_{s1} are determined as the slope of the swelling line at constant suction (s_1). In the meantime, parameters λ_{s2} and N_{s2} are obtained from the slope and the intercept of compression line at constant suction (s_2). Parameter κ_{s2} is determined from the slope of the swelling line at the constant suction (s_2).

For obtaining the two parameters related to the critical swelling–shrinkage line and two parameters related to the swelling stable line, the cyclic wetting–drying tests should be conducted. Based on the test results, the critical swelling–shrinkage line and the swelling stable line can be determined. Then, parameters e_{rc} and λ_{cs} can be obtained from the intercept and the slope of the critical swelling–shrinkage line, respectively. Parameters e_{rs} and λ_{ss} can be obtained from the intercept and the slope of swelling stable line, respectively.

According to all the 10 parameters determined, the yield suction can be calculated by Eqs. (8) and (9).

The elastic compressibility coefficient κ_s can be determined from the equilibrium (final) stage of the soil experienced several suction cycles.

$$\kappa_{si} = \frac{de}{d \log(s)} = \frac{e_2 - e_1}{\log(s_2/s_1)} \quad (10)$$

where s_1 and s_2 are the highest and lowest suctions of the wetting and drying cycles processed. e_1 and e_2 are the void ratios corresponding to suctions s_1 and s_2 , respectively. e_1 and e_2 can be calculated by Eqs. (3) and (4), respectively. Based on these, Eq. (10) is rewritten as:

$$\kappa_{si} = \frac{(\lambda_{ss} - \lambda_{cs}) \times \ln(p) + (e_{rs} - e_{rc})}{\log(s_2/s_1)} \quad (11)$$

Based on Eq. (11), the elastic compressibility coefficient κ_{si} can be calculated using parameters e_{rc} , λ_{cs} , e_{rs} and λ_{ss} .

In the meantime, the plastic compressibility coefficient λ_s can be determined from the elastic compressibility coefficient and the state parameter. The equation for

calculation of the plastic compressibility coefficient are assumed as,

$$\lambda_s = \begin{cases} \kappa_s [1 + (e_{cs1} - e)(e_{rc} - e)] & \text{wetting process} \\ \kappa_s [1 + (e_{ss1} - e)(e_{rs} - e)] & \text{drying process} \end{cases} \quad (12)$$

where the e_{cs1} is the critical void ratio, the e_{ss1} is the swelling stable void ratio.

5 Model verification

In order to evaluate the performance of the proposed model, the cyclic suction-controlled tests conducted on compacted bentonite [20] were simulated and analyzed.

5.1 Cyclic wetting–drying tests conducted on GMZ bentonite

Zhao et al. [20] conducted suction-controlled cyclic wetting–drying tests on compacted GMZ bentonite, which has some basic physical properties including a liquid limit 93%, a plastic limit 47% and a solid particle density 2.67 g/cm³. The statically and one-dimensionally compacted specimens (50 mm in diameter and 10 mm high) have dry densities 1.3 g/cm³, 1.5 g/cm³ and 1.7 g/cm³, respectively. All the specimens have an initial suction 110 MPa. The cyclic wetting–drying tests were conducted with suction changing between 0 MPa and 110 MPa under a vertical stress 50 kPa, 100 kPa, 200 kPa, 300 kPa or 400 kPa, respectively.

With the oedometer tests conducted under saturated condition [21] and the constant suction 110 MPa, the model parameters were obtained, respectively (Table 1).

Table 1 Parameters of GMZ bentonite

Parameter	Value
e_{rc}	2.19
λ_{cs}	0.28
e_{rs}	2.93
λ_{ss}	0.348
N_{s1}	1.43
λ_{s1}	0.281
κ_{s1}	0.024
N_{s2}	10.18
λ_{s2}	1.22
κ_{s2}	0.016

5.2 Simulation results and discussion

With parameters listed in Table 1, the swelling and shrinkage deformations were calculated and compared to the tested results (Fig. 7). Results in Fig. 8 show that the tested results could be reasonably described by the proposed model.

Results in Fig. 7 show that the difference between the swelling deformation on wetting process and the shrinkage deformation on the drying process was observed during each wetting–drying cycle. However, after four wetting–drying cycles, the swelling deformation and the shrinkage deformation are almost the same, indicating that the swelling–shrinkage deformation is reversible.

In the meantime, for the specimen with an initial dry density 1.3 g/cm^3 tested under the vertical stress 50 kPa, an accumulative swelling deformation was recorded (Fig. 7a). However, for the specimen with an initial dry density 1.5 g/cm^3 tested under the vertical stress of 400 kPa, an accumulative shrinkage deformation was recorded

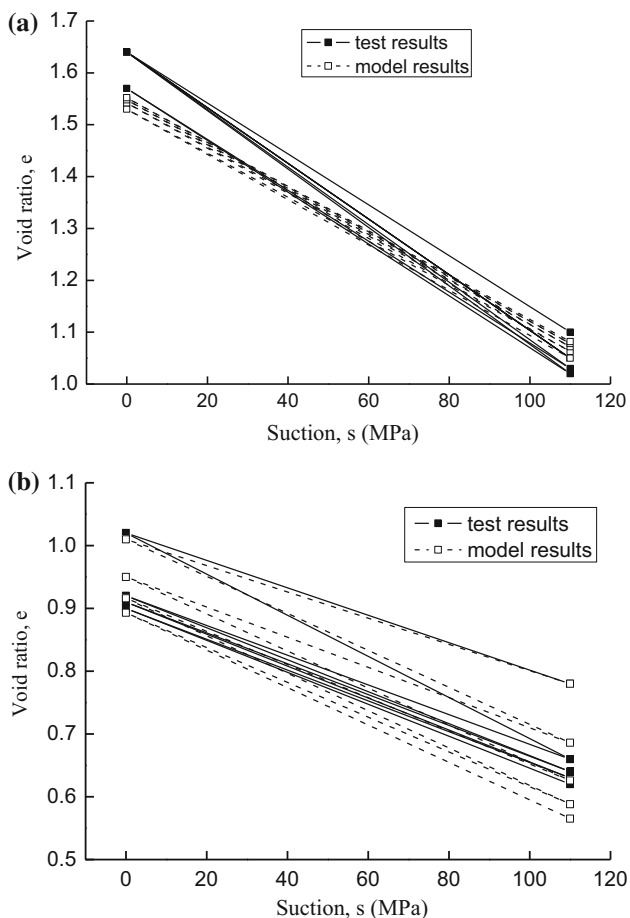


Fig. 7 Simulation of the specimens with initial dry density of 1.3 g/cm^3

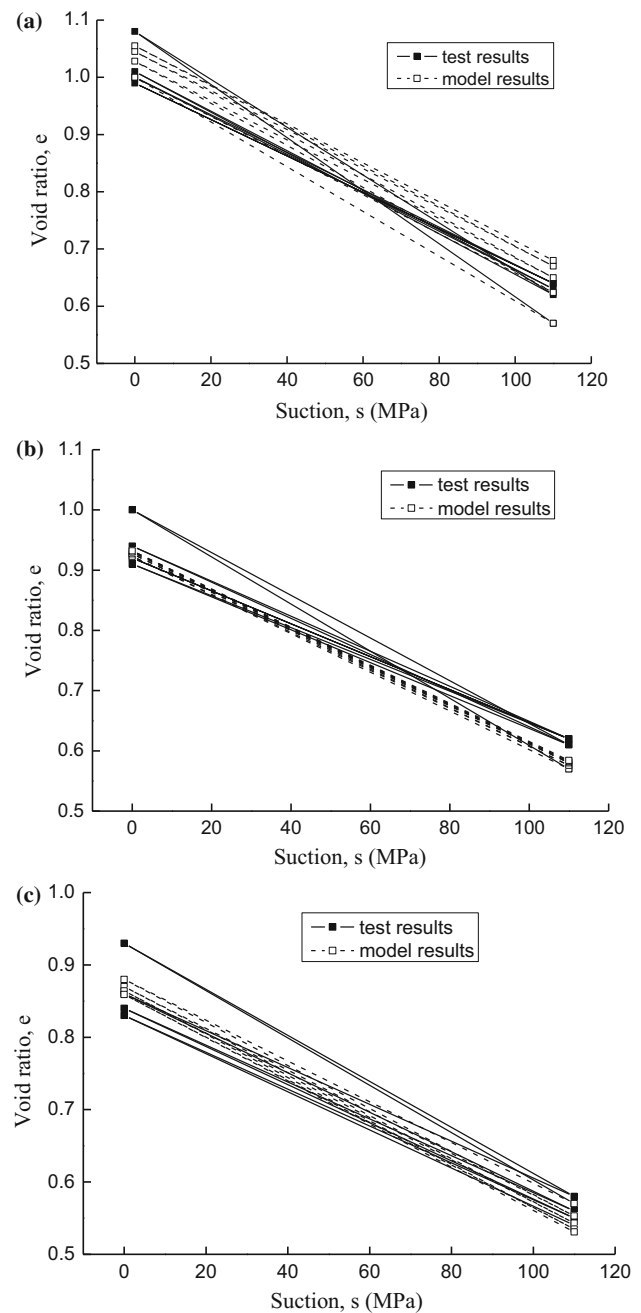


Fig. 8 Simulation of the specimens with initial dry density of 1.7 g/cm^3

(Fig. 7b). Moreover, all the accumulative deformations for the specimens tested increased with cycles.

For specimens tested under different vertical stresses, test results and related simulated results were compared in Fig. 8. Results in Fig. 8 show that the proposed model could reasonably describe the influences of the vertical stress on the accumulative deformation.

For specimens tested under the vertical stress 200 kPa and 300 kPa, accumulative swelling deformations were recorded (Figs. 8a and 8b). For the specimen tested under

the vertical stress of 400 kPa, an accumulative shrinkage deformation was recorded (Fig. 8c).

Test results of specimens with different initial dry densities were simulated (Fig. 9). Results also show that simulated results agree well with the tested ones, indicating that the effect of initial dry density on accumulative deformation could be reasonably described by the proposed model.

For the specimen with a dry density of 1.3 g/cm^3 , an accumulative shrinkage deformation was sped (Fig. 9a).

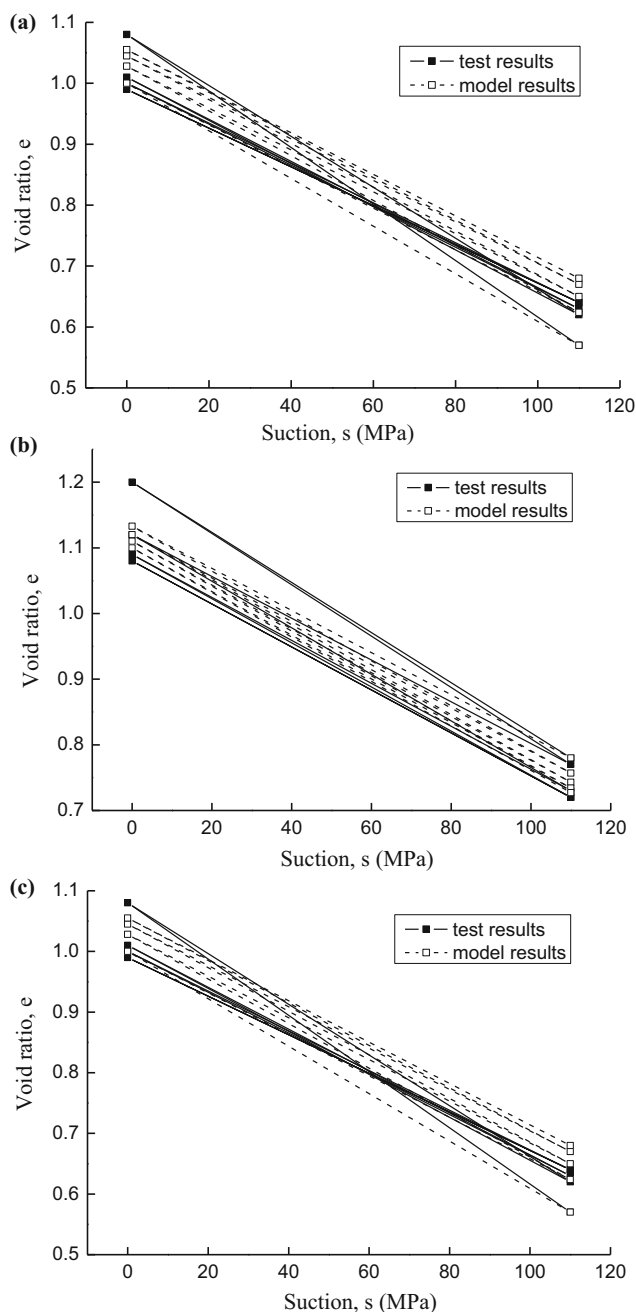


Fig. 9 Simulation of the specimens under the vertical stress of 200 kPa

For specimens with the dry density 1.5 g/cm^3 and 1.7 g/cm^3 , accumulative swelling deformations were recorded (Figs. 9b and 9c).

6 Conclusions

To simulate the volume change behavior of compacted expansive soil during wetting–drying cycles, a new constitutive framework was proposed. The concept of critical swelling–shrinkage state, which includes the elastic stable line, elastic zone, and state parameter, was analyzed. Then, a new suction decreasing yield surface and new suction increasing yield surface were proposed. For SD yield surface, the yield suction during wetting process decreases as the stress applied increases in the swelling zone and increases as the stress applied increases in the shrinkage zone. For SI yield surface, the yield suction during wetting process increases as the stress applied increases in the swelling zone and decreases as the stress applied increases in the shrinkage zone. Variations of the suction decreasing yield surface and suction increasing yield surface were described. The swelling stable stress, critical swelling–shrinkage stress, and yield stress were defined as hardening parameters. Based on these, a constitutive model was proposed. The calibration of the model was conducted. Comparisons between the simulation results and experimental data show that the proposed model can well describe the swelling–shrinkage behavior of compacted GMZ bentonite during the wetting and drying cycles.

It should be noted that, during the cyclic wetting–drying processes for soil tested under isotropic or oedometer conditions, the most important feature concerned is the swelling–shrinkage volume change. The model developed in this work is more suitable for describing the volume change behavior of expansive soils during cyclic wetting–drying processes.

Acknowledgements The authors are grateful to the National Natural Science Foundation of China (41672271, 41527801) for the financial supports. The authors also wish to acknowledge the support of the European Commission via the Marie Curie IRSES project GREAT–Geotechnical and geological Responses to climate change: Exchanging Approaches and Technologies on a world-wide scale (FP7-PEOPLE-2013-IRSES-612665).

References

- Airò Farulla C, Ferrari A, Romero E (2010) Volume change behaviour of a compacted scaly clay during cyclic suction changes. *Can Geotech J* 47(6):688–703
- Alonso EE, Gens A, Josa A (1990) A constitutive model for partially saturated soils. *Géotechnique* 40(3):405–430

3. Alonso EE, Vaunat J, Gens A (1999) Modelling the mechanical behaviour of expansive clays. *Eng Geol* 54:173–183
4. Alonso EE, Romero E, Hoffmann C, García-Escudero E (2005) Expansive bentonite-sand mixtures in cyclic controlled-suction drying and wetting. *Eng Geol* 81:213–226
5. Basma AA, Al-Homoud AS, Husein Malkawi AI, Al-Bashabsheh MA (1996) Swelling-shrinkage behavior of natural expansive clays. *Appl Clay Sci* 11(2):211–227
6. Chen FH (1988) *Foundations on expansive soils*. Elsevier, New York
7. Day RW (1994) Swell-shrink behavior of compacted clay. *J Geotech Eng* 120(3):618–623
8. Gens A, Alonso EE (1992) A framework for the behavior of unsaturated expansive clays. *Can Geotech J* 29(6):1013–1032
9. Hen-Jones RM, Hughes PN, Stirling RA, Glendinning S, Chambers JE, Gunn DA, Cui YJ (2017) Seasonal effects on geophysical-geotechnical relationships and their implications for electrical resistivity tomography monitoring of slopes. *Acta Geotech* 12:1159–1173
10. Li ZS, Benchouk A, Derfouf FM, Abou-Bekr N, Taibi S, Soili H, Fleureau J (2018) Global representation of the drying-wetting curves of four engineering soils: experiments and correlations. *Acta Geotech* 13:51–71
11. Nowamooz H, Masrouri F (2008) Hydromechanical behavior of an expansive bentonite/silt mixture in cyclic suction-controlled drying and wetting tests. *Eng Geol* 101:154–164
12. Nowamooz H, Mrad M, Abdallah A, Masrouri F (2009) Experimental and numerical studies of the hydromechanical behaviour of a natural unsaturated swelling soil. *Can Geotech J* 46(4):393–410
13. Nowamooz H, Masrouri F (2010) Influence of suction cycles on the soil fabric of compacted swelling soil. *Comptes Rendus Geosci* 342(12):901–910
14. Tang C, Shi B (2011) Swelling and shrinkage behaviour of expansive soil during wetting-drying cycles. *Chin J Geotech Eng* 33(9):1376–1384 (in Chinese)
15. Tripathy S, Subba Rao KS, Fredlund DG (2002) Water content-void ratio swell-shrink paths of compacted expansive soils. *Can Geotech J* 39(4):938–959
16. Tripathy S, Subba Rao KS (2009) Cyclic swell-shrink behaviour of a compacted expansive soil. *Geotech Geol Eng* 27(1):89–103
17. Wang G, Wei X (2014) Modeling swelling-shrinkage behavior of compacted expansive soils during wetting-drying cycles. *Can Geotech J* 47(6):688–703
18. Wei X, Duc M, Hattab M, Reuschlé TS, Fleureau J (2017) Effect of decompression and suction on macroscopic and microscopic behavior of a clay rock. *Acta Geotech* 12:47–65
19. Ye WM, Borrell NC, Zhu JY, Chen B, Chen YG (2014) Advances on the investigation of the hydraulic behaviour of compacted GMZ bentonite. *Eng Geol* 169:41–49
20. Zhao NF, Ye WM, Chen YG, Chen B, Cui YJ (2017) Investigation on swelling-shrinkage behavior of unsaturated compacted GMZ bentonite on wetting-drying cycles. *Bull Eng Geol Environ*. <https://doi.org/10.1007/s10064-017-1095-3>
21. Zhang F (2017) Chemo-mechanical coupling effects on the volume change behaviour of compacted GMZ01 bentonite. PHD thesis, Tongji University, Shanghai

Publisher's Note Springer Nature remains neutral with regard to jurisdictional claims in published maps and institutional affiliations.